

Design and Evaluation of a 42 V Automotive Alternator with Integrated Switched-Mode Rectifier

S.C. TANG, D.M. OTTEN, T.A. KEIM, AND D.J. PERREAULT

MASSACHUSETTS INSTITUTE OF TECHNOLOGY
LABORATORY FOR ELECTROMAGNETIC AND ELECTRONIC SYSTEMS
CAMBRIDGE, MA 02139 USA

Abstract— This paper presents techniques for the design of high-power Lundell alternators with integrated switched-mode rectifiers. A multi-section stator winding and interleaved rectifier arrangement is introduced that enables high power levels to be achieved using small semiconductor devices, and which greatly reduces the output filter capacitor requirements. We also demonstrate control methods suited to this interleaved system. In addition to accurate closed-loop output voltage control, we introduce methods to provide (partial) synchronous rectification for reduced loss, and to provide tight load dump transient control. The proposed technology is validated in the design and experimental evaluation of a 42 V, 3.4 kW alternator with fully integrated power electronics and controls. The prototype alternator achieves approximately a factor of 2.1 increase in power and 1.6 increase in power density as compared to a conventional diode-rectified alternator.

I. INTRODUCTION

There is an emerging need for automotive generators that can provide higher output power and power density, improved efficiency, and better transient response (including load dump suppression.) Moreover, there is an interest in developing electrical systems at a higher voltage (42 V) to better accommodate more electrical power in automobiles, and to achieve economies available through tighter suppression of overvoltage transients. These challenges have motivated a variety of research into automotive alternator design in recent years (e.g., [1-26]).

Previous work has shown that switched-mode rectification coupled with appropriate controls can provide dramatic improvements in the power capability, efficiency, and transient response of both Lundell and permanent magnet alternators [10-19, 24-26]. This paper carries this strategy forward, and presents the design and experimental evaluation of a high-power 42 V Lundell alternator having the power electronics and control circuitry fully integrated with the machine. The new design is shown to provide ~100% increase in output power and power density over a conventional alternator design, along with significant improvements in load dump transient performance. To achieve this, we introduce a multi-section winding and interleaved rectifier arrangement that enables high power levels to be achieved using small semiconductor devices, and which greatly reduces the output filter capacitor requirements. We also demonstrate control methods suited to this

interleaved system. In addition to accurate closed-loop output voltage control, we introduce means to provide (partial) synchronous rectification for reduced loss, and demonstrate the ability to achieve tight load dump transient control within the requirements of 42 V electrical systems [27].

The paper is organized as follows: Section II reviews the general principles underlying the alternator design, and introduces the interleaved winding and switched-mode rectifier structure we propose. The physical construction of the alternator system and integrated electronics is also described. Section III describes the control approach utilized with the interleaved architecture. Means for providing output voltage control are described, along with means for implementing synchronous rectification of the active devices. Experimental results demonstrating the efficacy of the control implementation are also presented. The load dump protection control scheme implemented in the system is also described, along with experimental results demonstrating the ability to meet the requirements of 42 V systems. Finally, Section IV concludes the paper.

II. SYSTEM CONFIGURATION

A. Switched-Mode Rectification and Load-Matching Control

Conventional three-phase Lundell alternators employ a diode bridge to rectify the generated ac voltages, and regulate the output voltage via field control. By exchanging the diodes in the bottom half of the rectifier bridge for active devices such as power MOSFETs, a semi-bridge switched-mode rectifier (SMR) is obtained (Fig. 1). The switched-mode rectifier provides additional means of controlling the alternator. As shown in [10] and elsewhere, by modulating the switches with an appropriate duty ratio (at a high frequency compared to the machine electrical frequency), the alternator output characteristics can be matched to the output in a manner that provides greatly increased power capability and efficiency across speed and power.

As shown in [10], the output power of an alternator with this SMR can be found as:

$$P_{out} = \frac{3(1-d)V_o}{\pi} \sqrt{\frac{(k\omega i_f)^2 - \left(\frac{2(1-d)V_o}{\pi}\right)^2}{\omega L_s}} \quad (1)$$

Where

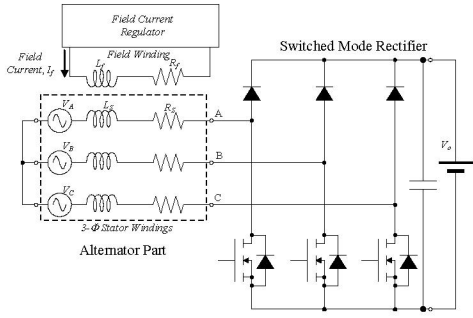


Figure 1 Alternator with a semi-bridge switched-mode rectifier.

P_{out} is the alternator output power
 d is the duty ratio of the active switches
 L_s is the synchronous inductance of the stator winding
 ω is the alternator angular electrical frequency
 i_f is the alternator field current, and
 k is the machine constant (line-neutral back EMF voltage magnitude $V_s = k \cdot \omega \cdot i_f$)

To obtain improved performance, duty ratio d is controlled up to a maximum value that provides load matching of the alternator (maximizing P_{out} in (1)):

$$d_{match} = 1 - \frac{\sqrt{2\pi k}}{4V_o} \omega i_f \quad (2)$$

By selecting appropriate combinations of duty ratio and field current, the alternator output power can be controlled up to a maximum that is a function of the alternator speed. The machine stator winding (which influences k and L_s) is selected to provide the desired capability for a specified output voltage V_o (e.g., 14 V or 42 V)¹. Figure 2 shows the output power capability for the prototype Lundell machine (for an appropriate stator winding) with both diode rectification and load matched operation (as with switched-mode rectification). As can be seen, the additional flexibility provided by the switched mode rectifier yields tremendous improvements in output power capability across the speed range. Moreover, as shown in [10], this can be achieved at higher efficiency and lower operating temperatures.

B. An Interleaved Alternator Design

While the use of switched-mode rectification offers major opportunities, it also poses some practical challenges. One issue to be addressed is the pulsating ripple current at the output of the switched-mode rectifier. Unlike a diode rectifier, the output current of the SMR of Fig. 1 pulsates at the switching frequency, yielding an RMS ripple current into the rectifier output capacitor that is on the order of $I_o \cdot (d/(1-d))^{1/2}$, where I_o is the average alternator output current. Low equivalent-series-resistance (ESR) capacitors with high ripple current rating are, therefore, required to absorb this ripple current and contribute to EMI filtering. This is certainly

¹ Neglecting device drops and other second-order effects, the same power capability can be achieved at any specified output voltage V_o by an appropriate rewinding of the stator.

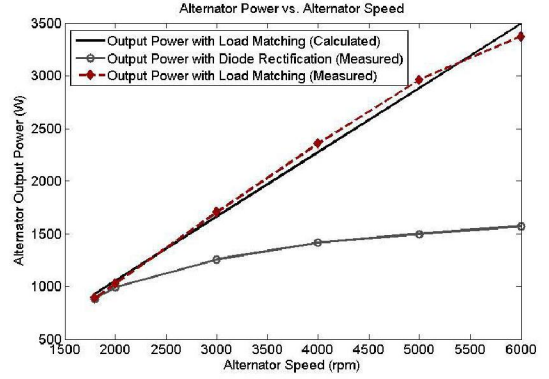


Figure 2 Alternator power capability vs. speed for diode rectification and for load matching control (e.g., with a switched-mode rectifier). Measured curves are for the alternator machine used in the prototype.

achievable in a small volume using film or multi-layer ceramic capacitors (see, e.g., [10]), but does represent a significant cost element. A second challenge relates to sizing of the semiconductor switches. At 14 V output, reasonably high-power alternators can be implemented with single-die plastic-packaged devices, owing to the wide availability of low-resistance 30 V and 20 V MOSFETs for low-voltage applications. At 42 V output, however, it is more difficult to realize the circuit of Fig. 1 without resorting to paralleled devices or devices modules (as used in [10]), especially when seeking to achieve high output power and temperature ratings.

Here we demonstrate a design strategy that addresses both of the above challenges. Instead of the design of Fig. 1, we employ an interleaved machine and rectifier configuration, as illustrated in Fig. 3. In this approach, the system is constructed from a number N_C of small rectifier cells connected in parallel, with each cell fed from a separate

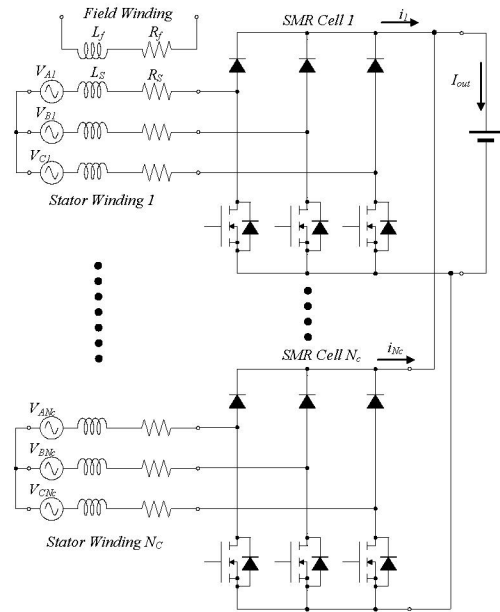


Figure 3 Schematic of multi-winding machine and interleaved switched-mode rectifier.

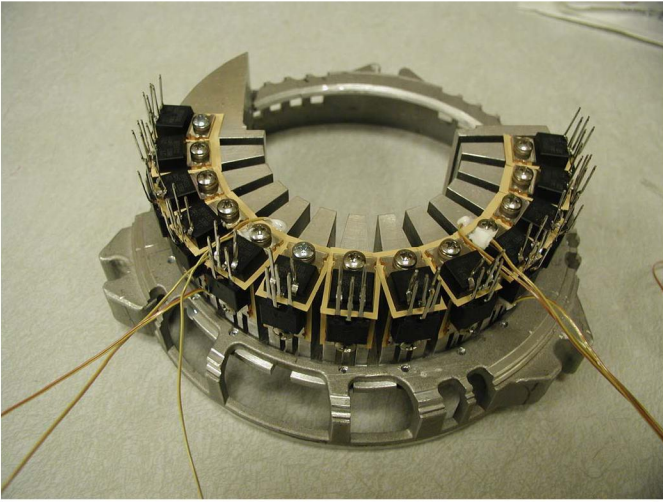


Figure 4 Switching devices and heat sink for the prototype 4-cell switched-mode rectifier system. The printed circuit board containing drive, control, and filtering circuitry mounts over this assembly.

isolated three-phase stator winding. The total system size and rating remains essentially unchanged, but utilizes more and smaller devices and windings. The switching patterns of the SMR cells are identical, but are each shifted in time from the other cells by T_{sw}/N_C , where T_{sw} is the SMR switching period. As will be shown, this provides significant advantages in filtering of the output. Interleaving has been previously applied in a variety of applications, including dc-dc converters [28, 29], rectifiers [30, 31], and even in alternators [5] (albeit with different operating conditions and design objectives).

Interleaving has a number of advantages in the present design. First, high power can be achieved using multiple rectifier cells, each of which only require small, single die devices in inexpensive packages. Moreover, the dissipation associated with rectification can be physically spread over a larger heatsink area, reducing the thermal management challenge. This can be seen qualitatively in the photograph of the distributed rectifier in our prototype system (Fig. 4.) A further major advantage of interleaving is the achievable reduction in output ripple and current rating of the output capacitor. Similar to the single SMR, each of the SMR cells delivers currents pulsating at the switching frequency. With interleaving, however, the *net* switching ripple current has a higher fundamental frequency (by a factor N_C) and its rms value is greatly reduced. This both greatly eases filtering of the output (e.g., to meet EMI specifications) and reduces the rms ripple rating of the alternator output capacitance. The degree to which ripple is attenuated depends on the number of cells employed and the duty ratio selected; the impact of this on control is considered in the next section.

C. Alternator Winding Design

The design described here is based on a modified Delco/Remy 92319 alternator (12 V, 130 A rating). The stator of the machine has 36 slots, into which the original three-phase winding was wave-wound. Each phase of the original machine comprised two parallel 14 AWG wires

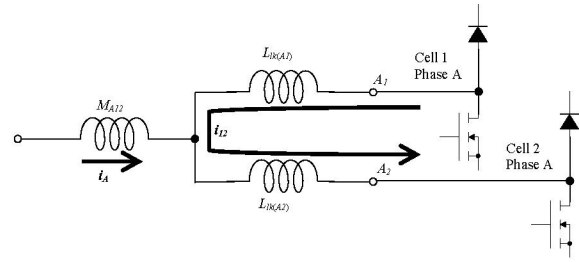


Figure 5 Equivalent circuit model illustrating circulating currents among different rectifier cells due to magnetic coupling among the phase sets.

wound for a total of 72 series turns, yielding six turns (12 wires) per slot, with some slots containing an additional two wires for terminating the winding. The stator was rewound for the proposed interleaved switched-mode rectifier system at 42 V output. Rewinding of the machine focused on realizing the multiple three-phase sets for an interleaved system (Fig. 3). A four-cell system was implemented having four separate sets of three-phase windings. Because our design incorporates a boost rectifier, the same number of turns (in each phase set) as the original 14 V alternator was used for 42 V output (see [10, 16, 25] for the impact of turns count). The machine was re-wound with each phase conductor comprising one strand of 17½ AWG wire, yielding a copper packing factor close to that of the original machine.

In implementing an interleaved system, the magnetic coupling among different winding sets must be carefully considered in order to prevent undesirable circulating currents and losses [25]. In particular, it is desirable for the individual stator sets to be magnetically isolated to a large extent, to prevent differential ac circulating current among cells. Fig. 5 uses an equivalent circuit incorporating a transformer T model to illustrate the impact of magnetic coupling between the two phase-A windings for SMR cells 1 and 2. Since the MOSFETs are switching on and off with a time shift, a differential ac voltage across terminals A_1 and A_2 results a circulating current i_{12} flowing through the winding leakage inductance, $L_{lk(A1)}$ and $L_{lk(A2)}$. This circulating current superimposes on the phase current, i_A , and causes ripple currents at the SMR cells inputs. The magnitude of i_{12} is inversely proportional to the values of $L_{lk(A1)}$ and $L_{lk(A2)}$. Thus, in a case when the phase windings are wound in the same stator slots, the large mutual coupling and small leakage inductance lead to a large value of circulating current and hence ripple currents at the SMR cells inputs.

To address the issue of magnetic coupling, the four sets of windings were wound in four separate sectors of the machine, as illustrated in Fig. 6. Each phase winding occupies a quadrant of the stator spanning 9 stator teeth. Because the number of slots for a phase winding is an odd number, windings of each phase in adjacent sectors share one stator slot. For example, as illustrated in Fig. 6, the two phase-A windings for SMR cells 1 and 2 share slot 10. As analyzed in detail in [25] and validated experimentally, this winding strategy limits magnetic coupling of different phase sets to a few percent, producing large leakage inductance and

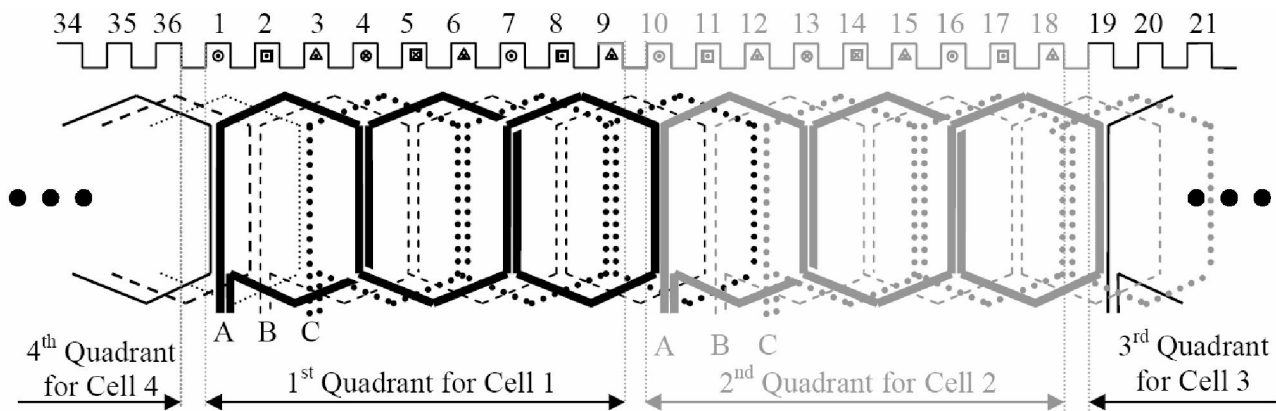


Figure 6 Stator winding configuration for the 4-SMR-cell alternator system. Each winding comprises 72 series turns made with $17\frac{1}{2}$ AWG wire (48 wires per slot). Adjacent sectors having different phase sets share only one slot, limiting magnetic coupling to a small value [25].

eliminating practical concerns about circulating current. The only disadvantage observed in this highly separated winding scheme is that any mechanical offset in the position of the rotor from the true center of the stator can yield differences in gap (and hence back emf) among different phase sets. The back emf variations that were encountered in practice were only on the order of 5%, however, which was found to be acceptable.

D. Rectifier Design and Integration

The rewound machine described above has been coupled with a four-cell ($N_C = 4$) switched mode rectifier (Fig. 3) to realize a 3.4 kW, 42 V alternator. This alternator has the power electronics and control circuitry fully integrated into the machine. To accommodate the prototype switched-mode rectifier, heat sink, and sensors, the alternator case was extended by approximately 4 cm (roughly by a factor of 1.3). As the redesigned alternator achieves a factor of 2.1 increase in output power (Fig. 2), we have achieved more than a factor of 1.6 improvement in power density. (Based on our subsequent work, we believe that the rectifier could be incorporated with *no* increase in case length, promising over a factor of two improvement in power density.) A photograph of the prototype alternator (with thermocouples attached and internal node voltages brought out) is shown in Fig. 7.

Based on our design studies (including [17, 23-26]), it is expected that a three-cell interleaved design would have been adequate for meeting the target performance and semiconductor thermal requirements to ambient temperatures beyond 85 °C. However, we developed the four-cell design in to make better use of the available heat sink area and achieve higher temperature capability. Each of the four cells utilizes three IRFB4310 MOSFETs (100 V, 5.6 m Ω , T0-220 package) and three 30CTQ100 Schottky diode pairs (100 V, 2 x 30 A, T0-220 package), locally bypassed with three 0.47 μ F ceramic capacitors. Note that the voltage ratings of the semiconductor devices were selected quite conservatively, as testing demonstrated that voltage transients could be limited below 56 V even under load dump conditions (see Section III). The MOSFETs are driven from IR4426S gate drivers via 4.7 Ω

series resistors. Control is provided by a MC68HC908 Microcontroller which controls both the switched-mode rectifier and provides PWM field control. The switched-mode rectifier operates at a switching frequency of 100 kHz, representing a reasonable tradeoff between switching and conduction loss, while the field is pulse-width modulated at 12.5 kHz. A custom aluminum heat sink was designed based on thermal models for the alternator developed in [17, 23]; a photograph of the devices mounted to the heat sink is shown in Fig. 4. Acceptable temperature rises at the device cases of less than 50 °C were found for all operating conditions evaluated. Further details of the electrical and thermal design and testing of the switched-mode rectifier may be found in [23-26].

III. CONTROL

Control of the alternator encompasses a number of tasks. Foremost is the regulation of the output voltage across variations in load. This is achieved through control of both



Figure 7 The prototype 4-cell alternator. The 42 V alternator and power electronics are completely integrated. Numerous voltages and temperatures are brought out for evaluation purposes.



Figure 8 The experimental setup used to test the prototype system. The system enables measurement of voltages, currents, and temperatures across a wide range of drive and load conditions. Details of the experimental apparatus and methods may be found in [26].

the alternator field current and the switching pattern of the rectifier. Control of the field and switched-mode rectifier should also be performed in a manner that meets other goals, such as maintaining high efficiency and controlling output ripple. Additionally, there is a need to handle fault conditions. One requirement is to limit the “load dump” voltage transient that can occur when the battery is suddenly disconnected from the alternator while drawing high current [34-43]. In this section we describe how these control requirements are addressed in the prototype system, and present experimental results that validate our methods. A photograph of the experimental setup is shown in Fig. 8.

A. Switched-Mode Rectifier Control

Multiple possibilities exist for controlling the output voltage and current of the interleaved alternator configuration of Fig. 3. In each case, one selects a combination of field current and duty ratio that provides sufficient power to regulate the output. One straightforward possibility is to operate the interleaved system exactly as a single-cell design, but with the gating waveforms of the cells interleaved appropriately. For example, one might select the field current and duty ratio according to the efficiency-optimizing controller of [10], and simply phase shift the gating waveforms to the individual cells by appropriate amounts. With this strategy, the switching ripple current into the output capacitor is reduced by an amount that depends on the number of cells and the duty ratio, and the fundamental switching ripple frequency is increased by a factor N_C (e.g., see [25, 28-33]).

Another control possibility arises from the fact that the switching ripple currents delivered by the interleaved cells cancel completely for certain duty ratios (e.g., see [25, 28-30]), yielding an output waveform that is ideally free of switching ripple. For example, as illustrated in Fig. 9, in a

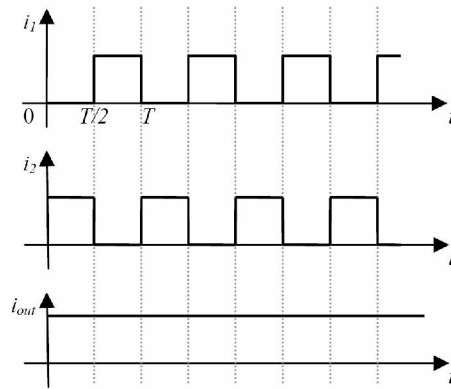


Figure 9 Example of ripple cancellation with interleaving for two interleaved cells.

two-cell system operating at a 50% duty ratio ($d = 0.5$), the pulsating currents from the individual cells add to provide a continuous (small-ripple) output current waveform. Thus, a two-cell system can ideally be operated at $d = 0$ (corresponding to diode rectification) or $d = 0.5$ with minimal switching ripple. Likewise, in a four-cell system ($N_C = 4$), the cell switching ripple currents cancel completely for duty ratios d of 0, 0.25, 0.5, and 0.75. By accepting operation at only these specific duty cycles, significant reductions in capacitor rating and filtering requirements can be achieved at the expense of design complexity.

The alternator design demonstrated here takes advantage of this “perfect cancellation” interleaving strategy. Because we constrain the control to only discrete duty ratios, the load matching condition indicated in (2) and illustrated in Fig. 2 is not achieved precisely across speed. However, in our four-cell design there is sufficient flexibility with four available duty ratios ($d = 0, 0.25, 0.5$ and 0.75) to make a reasonable approximation to load-matched performance at heavy loads. Fig. 10 shows experimental measurements of alternator output power at full field current and at each of these duty ratios across speed. Fig. 11 demonstrates automatic duty ratio switching to achieve near load-matched power across speed; the two curves illustrate performance for increasing and decreasing speed, respectively.

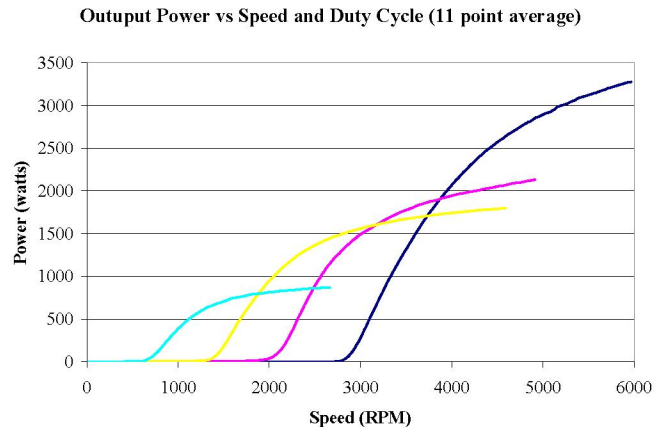


Figure 10 Experimental output power at full field and each allowed duty ratio (rising from left to right: $d = 0.75, 0.5, 0.25$, and 0).

Alternator Output Power vs Speed @ 3.6A Field Current

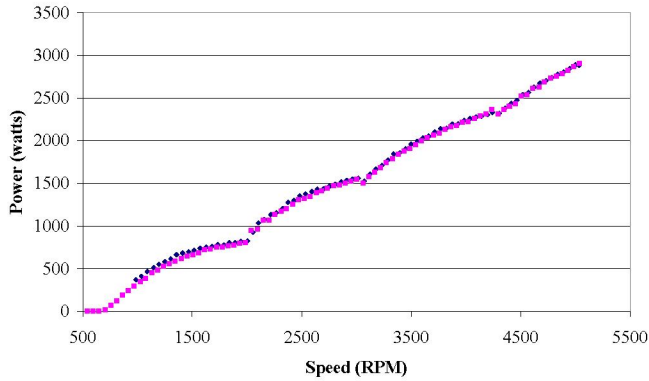


Figure 11 Experimental output power at full field with automatic duty-ratio switching. Dark dots are for rising speed, light dots are for falling speed.

B. Output Voltage Regulation

Given the selected restriction to a discrete set of SMR duty ratios for ripple cancellation, the question arises of how to maintain output regulation across alternator speed and load. The strategy adopted in our prototype system is to select an appropriate duty ratio based on alternator speed (with a small amount of hysteresis in the transition points), and to regulate the output power within that speed range via field control. Table 1 shows the transition speeds for switching among the allowed duty ratios, and illustrates the hysteresis in the transitions.

In realizing this control scheme, there is a need to detect the alternator speed. Figure 12 illustrates the method and circuitry for detecting alternator speed. The pulsating voltage at the drains of three SMR MOSFETs is measured and filtered to provide a set of digital signals. Each signal indicates the direction of the current of that alternator phase. By measuring the period of the signals, the electrical frequency and alternator speed is easily determined. Moreover, these signals can be used for implementing partial synchronous rectification (as described below).

Alternator field current is adjusted between 0 and a maximum value (nominally 3.6 A) by pulse-width modulation. As the field is wound for a 14 V output but is driven from 42 V in our design, the field duty ratio is limited to a maximum value of 28% (below 33%). Field duty ratio is adjusted based on output voltage error mainly via proportional control, with a voltage deviation of +/-2.68 V causing a field

Transition Table		
Duty Cycles	Transition Speed for Decreasing d	Transition Speed for Increasing d
0.5, 0.75	2001 rpm	1744 rpm
0.25, 0.5	3212 rpm	2839 rpm
0, 0.25	4360 rpm	3938 rpm

Table 1 Transition speeds for increasing and decreasing the switched-mode-rectifier duty ratio.

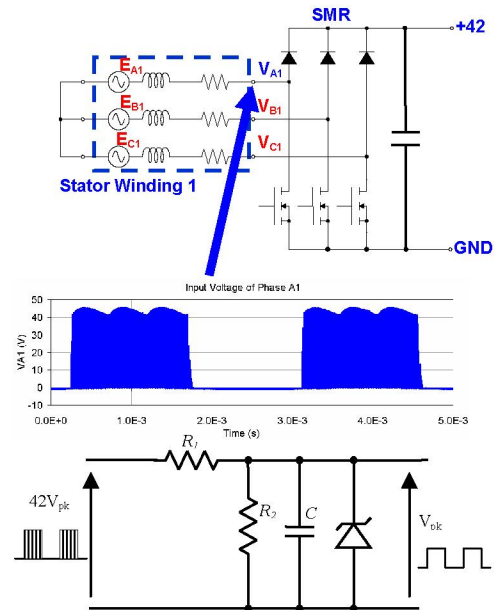


Figure 12 Circuit and method for detecting alternator speed and phase current direction. This information is used in controlling the SMR duty ratio and implementing synchronous rectification.

duty ratio swing between zero and maximum. A small summed error term (digital integral term) is also added into the field duty ratio to provide good steady-state performance, but the gain of this integral term is sufficiently small that it does not compromise the dynamics of the proportional control.

Figure 13 shows how field current varies as a function of speed to maintain the desired output at a variety of loads ranging from 100 W to 2500 W. The speed points where the duty ratio transitions occur are clearly visible. Figure 14 shows output power vs. speed for the alternator for a number of fixed load currents. Notice how the effect of duty ratio transitions and field current variations and transitions cancel to produce the desired constant power across speed. Figure 15 shows a scatter plot of the alternator output voltage across speed and load power; almost all of the points fall within +/-

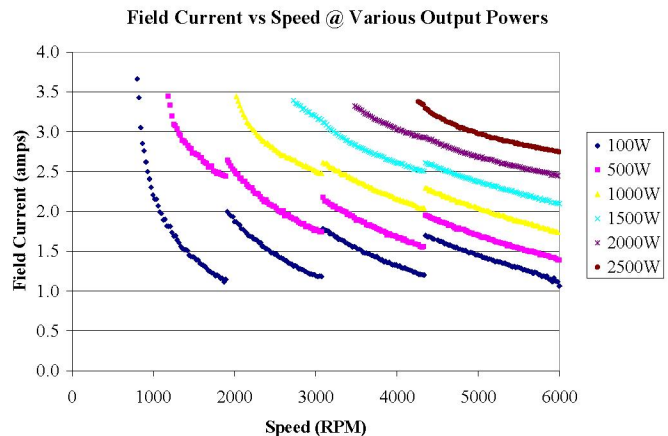


Figure 13 Experimental measurement of field current (scale 0 – 4 A) vs. alternator speed at various output power levels (100 W, 500 W, 1000 W, 1500 W, 2000 W, 2500 W).

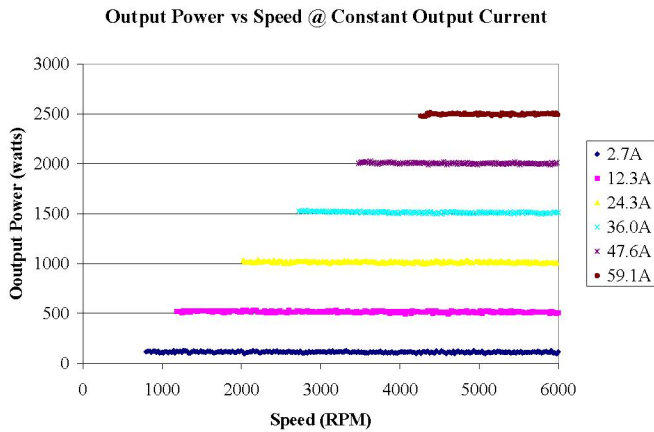


Figure 14 Experimental measurement of output power (scale 0 – 3000 W) vs. alternator speed at various load current levels (2.7 A, 12.3 A, 24.3 A, 36.0 A, 47.6 A, 59.1 A).

0.4 V of the setpoint of 42.0 V. These results demonstrate the ability to regulate the output across a wide speed and load range with the proposed control approach.

C. Synchronous rectification

In order to maintain high efficiency, it is desirable to achieve at least partial synchronous rectification with the MOSFETs in the switched-mode rectifier. That is, in order to reduce loss we would like to turn the MOSFETs on when the phase currents would otherwise pass through the MOSFET body diodes. This requires some means to detect the direction of the phase current. We achieve this without the need for direct current measurements using the approach illustrated in Fig. 12 and described above. Figure 16 illustrates the pulsating drain voltage of the MOSFET along with the digital signal to the microprocessor indicating phase current direction. The digital signals indicating phase current direction are used to synthesize synchronous rectification pulses to hold the MOSFETs on during the appropriate time period. Note that when the MOSFET is held on, we cannot detect a direction change for the phase current with this

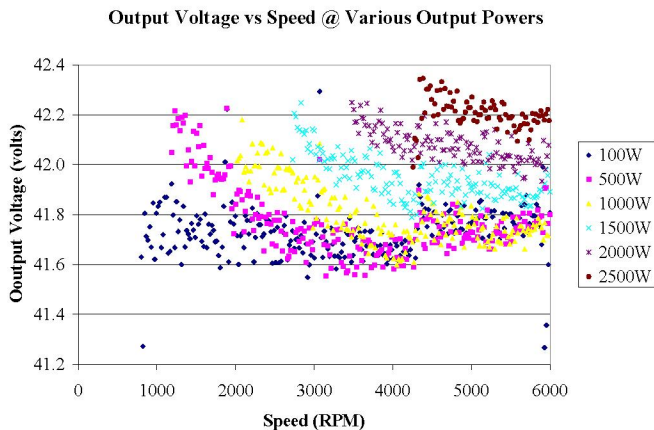


Figure 15 Experimental measurement of output voltage (scale 41.2 V – 42.4 V) across speed (scale 0 – 6000 RPM) at output power levels from 100 W to 2500 W.

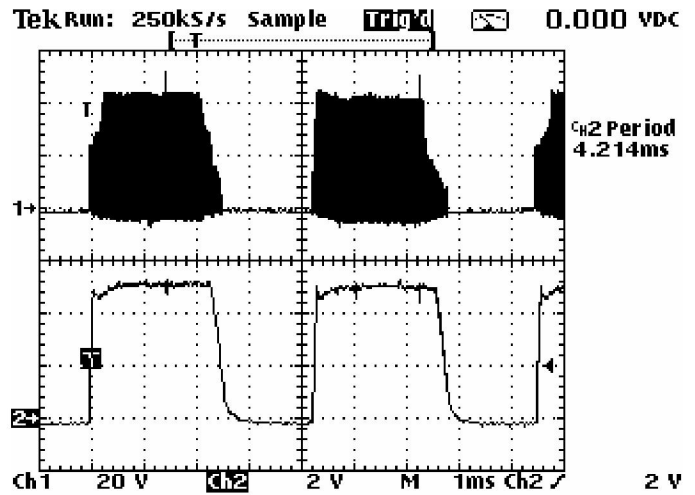


Figure 16 Experimental measurement of a MOSFET drain voltage (Ch. 1) and the digital phase current direction signal (Ch. 2) generated by the circuit of Fig. 12.

method. Because of this, and to accommodate the fact that the span of the desired on pulse varies with speed and load, we only set the synchronous rectification pulse width to 85% of the time indicated by our detection scheme, thus providing some operating margin. Moreover, whenever the alternator first starts up or changes duty ratio, the synchronous rectification pulses are turned off and then slowly increased to their 85% duration over a number of cycles. This allows efficient operation under steady-state conditions without causing problems during transients.

Testing of the proposed synchronous rectification scheme demonstrated its efficacy. It was found that synchronous rectification always provides an improvement in operating temperatures of the switched-mode rectifier. Considering the worst-case thermal points for the switched-mode rectifier at each duty ratio, it was found that synchronous rectification lowered diode temperature an average of 4.6 °C and MOSFET temperature an average of 7.4 °C (on the order of 10% of total temperature rise). Detailed measurements for a variety of operating conditions may be found in [26]. As there is no additional hardware expense and little control complexity to realizing the proposed synchronous rectification scheme, its use is well justified.

D. Load Dump Transient Control

Control of load-dump transients is another important aspect of alternator design. This is particularly important in 42 V electrical systems, since the proposed transient limits [27] are much tighter (on a percent overvoltage basis) than is typically achieved with Lundell alternators (e.g., see. [34-43]). The SMR alternator can achieve significantly improved output voltage transient response as compared to a diode rectified alternator [10]. When a load dump event takes place, the output current of the alternator has no place to go so the output voltage builds up. If the increase in output voltage is sensed, and the MOSFETs in the rectifier are turned on when the voltage exceeds a threshold, the alternator current can be

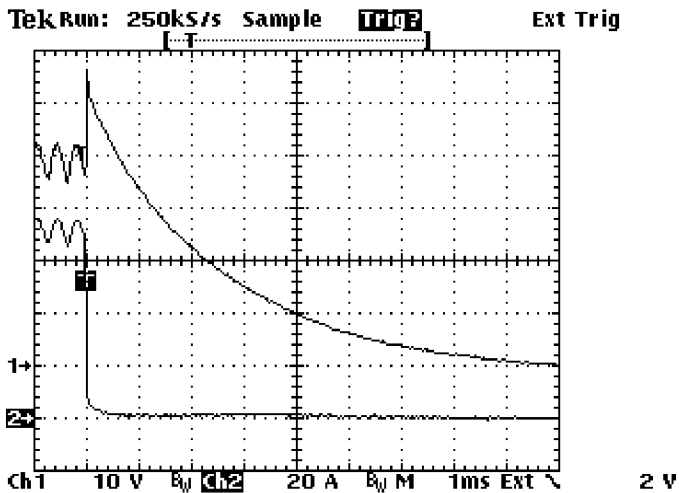


Figure 17 Load dump transient response for a load step from 0.58Ω to 42Ω ($\sim 3024 \text{ W}$ to $\sim 42 \text{ W}$) at 4500 rpm with no battery. Channel 1 shows alternator output voltage, while channel 2 shows alternator output current. The output voltage transient is limited to 58 V.

diverted from the output while the field current is reduced, and the high voltage transient associated with the energy stored in the machine synchronous reactance can be eliminated. Moreover, shorting the output of the machine via the MOSFETs prevents the line-to-line back emf voltage of the alternator from appearing at the rectifier output. The strategy undertaken is thus to detect the occurrence of a load dump transient overvoltage with a comparator. When a fault is detected, the SMR MOSFETs are turned on, and the field drive is turned off. After a minimum 300 mS delay for clearance of the fault, the alternator restarts.

To demonstrate this load dump control strategy, the output of the alternator was connected to a switched resistor network, without the presence of a battery or large capacitive filter. Only a small $60 \mu\text{F}$ capacitance was included at the alternator output in addition to the $6.1 \mu\text{F}$ of bypass capacitors on the SMR printed circuit board. The switched resistor network was configured to permit the load resistance to be rapidly switched from 0.58Ω to 42Ω (72 A to 1 A / 3024 W to 42 W).

Figure 17 shows example results for alternator operation at 4500 rpm (0% duty cycle) and an initial load 72 A. As the load dump is detected, alternator output current is cut off (diverted through the SMR MOSFETs). The transient voltage rises to a peak of approximately 58 V at a rate of about $1.3 \text{ V} / \mu\text{sec}$. Repeated testing demonstrated the ability to limit peak overvoltage at the alternator output to 58 V. Note that during the load dump suppression, the rectifier MOSFETs see higher than the usual current. Measurements of the MOSFET currents show that they peak at about 56 A, and decay approximately with the same time constant as the field current. As the MOSFETs in this design have a peak current rating of 140 A and the overcurrent lasts only a very short time (50-100 msec), there is no danger of damage to the alternator or the external system.

It may be concluded that tight load dump control is achieved in the prototype system. Control of the switched-mode rectifier under full-scale load dump transients yields a peak overvoltage of only 58 V on the 42 V system, without undue stress on the semiconductor devices.

IV. CONCLUSION

This paper presents techniques for the design of high-power Lundell alternators with integrated switched-mode rectifiers. A multi-section stator winding and interleaved rectifier arrangement is introduced that enables high power levels to be achieved using small semiconductor devices, and which greatly reduces the output filter capacitor requirements. We also demonstrate control methods suited to this interleaved system. In addition to accurate closed-loop output voltage control, we introduce methods to provide (partial) synchronous rectification for reduced loss, and to provide tight load dump transient control. The proposed technology is validated in the design and experimental evaluation of a 42 V, 3.4 kW alternator with fully integrated power electronics and controls. The prototype alternator achieves approximately a factor of 2.1 increase in power and 1.6 increase in power density as compared to a conventional diode-rectified alternator, along with a substantial improvement in load dump performance.

ACKNOWLEDGEMENTS

The authors would like to acknowledge the support for this research provided by the member companies of the MIT/Industry Consortium on Advanced Automotive Electrical/Electronic Components and Systems.

REFERENCES

- [1] G. Henneberger: "Improvement of the output performance of the claw-pole alternators by additional permanent magnets," *International Conference on Electric Machines (ICEM) '94*, Paris, France, 1994.
- [2] M. Naidu, M. Boules, and R. Henry: "A High Efficiency, High Power Generation System for Automobiles," *1995 IEEE Industry Applications Society Annual Meeting*, 1995, pp. 709-716.
- [3] F. Liang, J. Miller, and S. Zarei: "A Control Scheme to Maximize Output Power of a Synchronous Alternator in a Vehicle Electrical Power Generation System," *1996 IEEE Industry Applications Society Annual Meeting*, October 1996, pp. 830-835.
- [4] F. Liang, J. Miller, X. Xu: "A Vehicle Electrical Power Generation System with Improved Output Power and Efficiency," *IEEE Transactions on Industry Applications*, Vol. 35, No. 6, Nov./Dec. 1999, pp. 1341-1346.
- [5] H. Ishikawa, A. Umeda, and M. Kohmura: "Development of a More Efficient and Higher Power Generation Technology for Future Electrical Systems," SAE Paper 2000-01-C081, *2000 International Congress on Transportation Electronics (Convergence 2000)*, Detroit, MI, Oct. 2000.
- [6] A.L. Julian and G. Oriti: "New Brushless Alternator for Automotive Applications," *2001 IEEE Industry Applications Society Annual Meeting*, Sept./Oct. 2001, pp. 443 - 448.
- [7] I. Boldea, S. Scridon, and L. Tutelea: "BEGA- A biaxial excitation generator for automobiles," *Proceedings of the 7th International OPTIM Conference*, Brasov, Romania, May 10-11, 2000.

- [8] F.B. Reiter Jr., K. Rajashekara, and R.J. Krefta: "Salient Pole Generators for Belt-Driven Automotive Alternator Applications," *2001 IEEE Industry Applications Society Annual Meeting*, 2001, pp. 437-442.
- [9] S. Scridon, I. Boldea, L. Tutelea, F. Blaabjerg, and A.E. Richie: "BEGA - A Biaxial Excitation Generator for Automobiles: Comprehensive Characterization and Test Results," *IEEE Transactions on Industry Applications*, Vol. 41, No. 4, July-Aug. 2005, pp. 935 - 944.
- [10] D.J. Perreault and V. Caliskan: "Automotive Power Generation and Control," *IEEE Transactions on Power Electronics*, Vol. 19, No. 3, May 2004, pp. 618-630.
- [11] J.M. Rivas, D.J. Perreault, and T.A. Keim: "Performance Improvement in Alternators with Switched-Mode Rectifiers," *IEEE Transactions on Energy Conversion*, Vol. 19, No. 3, Sept. 2004, pp. 561-568.
- [12] W.L. Soong and N. Ertugrul: "Inverterless High-Power Interior Permanent-Magnet Automotive Alternator," *IEEE Transactions on Industry Applications*, Vol. 40, No. 4, July-Aug. 2004, pp. 1083 - 1091.
- [13] C.-Z. Liaw, D.M. Whaley, W.L. Soong, and N. Ertugrul: "Investigation of Inverterless Control of Interior Permanent-Magnet Alternators," *IEEE Transactions on Industry Applications*, Vol. 42, No. 2, March/April 2006, pp. 536-544.
- [14] C.Z. Liaw, W.L. Soong, and N. Ertugrul, "Closed-Loop Control and Performance of an Inverterless Interior PM Automotive Alternator," *2005 Conference on Power Electronics and Drive Systems*, pp. 343-348.
- [15] C.Z. Liaw, W.L. Soong, and N. Ertugrul, "Low-Speed Output Power Improvement of an Interior PM Automotive Alternator," *2006 IEEE Industry Applications Society Annual Meeting*, 2006, pp. 27-34.
- [16] G. Hassan, D.J. Perreault, and T.A. Keim, "Design of Dual-Output Alternators with Switched-Mode Rectification," *IEEE Transactions on Power Electronics*, Vol. 20, No. 1, Jan. 2005, pp. 164-172.
- [17] S.C. Tang, T.A. Keim, and D.J. Perreault: "Thermal Modeling of Lundell Alternators," *IEEE Transactions on Energy Conversion*, Vol. 20, No. 1, March 2005, pp. 25-36.
- [18] L.M. Lorilla, T.A. Keim, J.H. Lang, and D.J. Perreault: "Topologies for Future Automotive Generators, Part I: Modeling and Analytics," *2005 Vehicle Power and Propulsion Conference*, Chicago, IL, Sept. 2005.
- [19] L.M. Lorilla, T.A. Keim, J.H. Lang, and D.J. Perreault: "Topologies for Future Automotive Generators, Part II: Optimization," *2005 Vehicle Power and Propulsion Conference (VPP)*, Chicago, IL, Sept. 2005.
- [20] D.J. Perreault, T.A. Keim, J.H. Lang, and L.M. Lorilla, "Applications of Power Electronics in Automotive Power Generation," *SLA International Conference Automotive Power Electronics*, Paris, France, June, 2006.
- [21] L.M. Lorilla, T.A. Keim, J.H. Lang, and D.J. Perreault: "Foil Field Lundell Alternator with Rotating Power Electronics," *2006 IEEE Power Electronics Specialists Conference*, Jeju, Korea, June 2006, pp. 2164-2169.
- [22] S. Rees and U. Ammann, "A Smart Synchronous Rectifier for 12 V Automobile Alternators," *2003 IEEE Power Electronics Specialists Conference*, 2003, pp. 1516-1521.
- [23] S. C. Tang, D.J. Perreault, and T.A. Keim, "Advanced Automotive Power Electronics: Thermal Analysis of Lundell Alternator," Summer 2002 Project Report, MIT/Industry Consortium on Advanced Automotive Electrical/Electronic Components and Systems, September 2002.
- [24] S.C. Tang, D.J. Perreault, and T.A. Keim, "Advanced Automotive Power Electronics: Switching Behavior of Power MOSFETs in Switched-Mode-Rectifier for Lundell Alternator," Winter 2003 Project Report, MIT/Industry Consortium on Advanced Automotive Electrical/Electronic Components and Systems, January 14, 2003.
- [25] S.C. Tang, D.J. Perreault, and T.A. Keim, "Electronically-Aided Power Generation and Control: Design Principle of Interleaved Switched Mode Rectifier for Lundell Alternator," Summer 2003 Project Report, MIT/Industry Consortium on Advanced Automotive Electrical/Electronic Components and Systems, August 21, 2003.
- [26] David Otten, "Test Report: Switch Mode Rectifier Equipped Alternator," *MIT Laboratory for Electromagnetic and Electronic Systems*, September 2006.
- [27] J. M. Miller, D. Goel, D. Kaminski, H.-P. Schöner, and T. M. Jahns, "Making the case for a next generation automotive electrical system," SAE Paper 98C006, in *Proc. IEEE-SAE International Conference on Transportation Electronics (Convergence)*, Dearborn, MI, Oct. 1998, pp. 41-51.
- [28] C. Chang and M. Knights, "Interleaving technique in distributed power conversion systems," *IEEE Transactions on Circuits and Systems - I*, Vol. 42, May 1995, pp. 245-251.
- [29] D.J. Perreault and J.G. Kassakian, "Distributed Interleaving of Paralleled Power Converters," *IEEE Transactions on Circuits and Systems - I*, Vol. 44, No. 8, Aug. 1997, pp. 728-734.
- [30] B. A. Miwa, D. M. Otten, and M. F. Schlecht, "High efficiency power factor correction using interleaving techniques," *IEEE Applied Power Electronics Conf.*, Boston, MA, 1992, pp. 557-568.
- [31] B. A. Miwa, "Interleaved conversion techniques for high density power supplies," Ph.D. dissertation, Dept. of Electrical Engineering and Computer Science, Massachusetts Institute of Technology, June 1992.
- [32] B. N. Singh, G. Joos and P. Jain, "A new topology of 3-phase PWM AC/DC Interleaved Converter for Telecommunication Supply Systems," *2000 IEEE Industry Applications Society Annual Meeting*, Oct. 2000, pp. 2290-2296.
- [33] David J. Perreault and John G. Kassakian, "Design and evaluation of a cellular rectifier system with distributed control," *IEEE Transactions on Industrial Electronics*, Vol. 46, No. 3, June 1999, pp. 495-503.
- [34] D.J. Perreault, K.K. Afridi, and I.A. Khan, "Automotive Applications of Power Electronics," in *The Power Electronics Handbook*, M.H. Rashid, Ed., Academic Press, 2001, pp. 791-813.
- [35] SAE EMI Standards Committee (1995), "Immunity to Conducted Transients on Power Leads," SAE Standard J1113/11, in *SAE Handbook*, Society of Automotive Engineers, Warrendale, PA, 1999.
- [36] J.R. Morgan, "Transients in the Automotive Electrical System," *1973 Vehicular Technology Conference*, Cleveland, OH, pp.1-10.
- [37] S. Yamamoto, O. Ozeki, T. Yamanaka, and H. Kondo, "Electrical Environmental Characteristics for Automotive Electronic Systems," *IEEE Transactions on Vehicular Technology*, Vol. VT-32, No. 2, May 1983, pp. 151-157.
- [38] S. Korn, "Automobiles Need Transient Voltage Suppression," *Power Conversion and Intelligent Motion*, Vol. 15, No. 2, Feb. 1989, pp. 28-31.
- [39] T. Elfland, M. Manternach, A. Marshall, and J. Mings, "The Load Dump," *1990 IEEE Workshop on Electronic Applications in Transportation*, pp. 73-78.
- [40] J.D. Dimech, "Standardized Automotive Load Dump Testing," *1991 IEEE International Symposium on Electromagnetic Compatibility*, 1991, pp. 355-359.
- [41] P. Le Bars, "42 V Load Dump Transient and Centralised Active Suppression," *Passenger Car Electrical Architecture IEE Seminar*, London, UK, 2000, pp. 4/1-4/3.
- [42] C.S. Namuduri, B.V. Murty, and M.G. Reynolds, "Load Dump Transient Control of a 42V Automotive Generator," *2004 IEEE Power Electronics Specialists Conference*, Aachen, Germany, 2004, pp. 389-394.
- [43] Z.J. Shen, S.P. Robb, F.Y. Rob, M. Fuchs, D. Berels, and K. Hampton, "Load Dump Protection in 42 V Automotive Electrical Distribution Systems," *2001 IEEE Applied Power Electronics Conference*, 2001, pp. 289-295.